Available online http://amq.aiqua.it
ISSN (print): 2279-7327, ISSN (online): 2279-7335

Alpine and Mediterranean Quaternary, 34 (1), 2021, 165-180 https://doi.org/10.26382/AMQ.2021.11

THE FOSSILIZATION OF MAMMAL BONES AT LA POLLEDRARA DI CECANIBBIO (ROME, CENTRAL ITALY). INSIGHTS FOR IN SITU PRESERVATION.

Federica Marano[1], Maria Rita Palombo[2], Eugenio Cerilli[3], Salvatore Milli[4,2]

[1] Palaeontologist freelance, Roma, Italy.
[2] CNR-IGAG, Istituto di Geologia Ambientale e Geoingegneria, Monterotondo, Italy.
[3] Archaeozoologist freelance, Roma, Italy.
[4]Dipartimento di Scienze della Terra, SAPIENZA Università di Roma, Italy.

Corresponding author: Federica Marano <federica.marano86@gmail.com>

ABSTRACT: The identification of mineralogical and chemical composition of the fossil bones is essential for reconstructing the depositional paleo-environment and burial processes, and to highlight the mechanisms triggering the fossilization processes during diagenesis. At La Polledrara di Cecanibbio, (the richest Middle Pleistocene paleontological and archaeological deposit in central Italy), a museum exhibits in situ thousands of fossils deposited into a fluvial and fluvio-palustrine environment during Marine Isotope Stage 9. The aim of this research is to disentangling between the chemical modifications undergone by the bone tissues of La Polledrara di Cecanibbio mammal remains exposed *in situ* to environmental agents on the excavated surface and those undergone by bones kept or displayed in museums. X-ray Diffraction (XRD), Raman Spectroscopy and SEM-EDS analyses were carried out to establish the chemical composition of fossil bones and the alteration occurred over time. To estimate the trend of the environmental parameters inside the museum, the measures of the temperature, the relative humidity and the dew point were recorded during at least three seasons. Fluoroapatite is the principal mineral phase identified in the fossils, testifying that the fluoritisation of the hydroxylapatite is the main fossilization process at La Polledrara di Cecanibbio. Barite and gypsum are also present, in response to ground water qualities and geochemistry of the depositional and burial environment. In addition, efflorescences of gypsum crystals have been detected on the surface of fossil bones. The research performed at La Polledrara di Cecanibbio suggests that the crystallization of secondary minerals such as gypsum crystals depends on environmental conditions and the high solubility of this salt coupled with the facility of expansion upon its re-precipitation inside the bone tissues, constitute the main cause of deterioration. Therefore, the monitoring and stabilization of the indoor environmental parameters are essential for identifying the degradation potential factors and process of bone degradation. They represent the best protocol to follow for preserving *in situ* fossil bones.

Keywords: *Palaeoloxodon*, fossilization, preservation, geosite, Cultural Heritages.

1. INTRODUCTION

The determination of the chemical characteristics of bone and soft tissues of vertebrate remains retrieved from archaeological and palaeontological deposits could provide multiple clues in determining the biological aspect of animal life, the environments they inhabited, the impact due to human presence and anthropogenic activities, as well as the biostratinomic and diagenetic processes leading to their burial and fossilization (Lee-Thorp, 2002; Trueman & Tuross, 2002; Berna et al., 2004; Trueman et al., 2004; Kohn & Law, 2006; Clementz, 2012; Keenan et al., 2015; Jaouen & Pons, 2017; Silaev et al., 2017; Decrée et al., 2018; Ma et al., 2019; Diana et al., 2020; Manthi et al., 2020; and references therein).

The bone tissue is constituted by organic and inorganic components, primarily hydroxylapatite [$Ca_{10-x}(PO_4)_{6-x}(HPO_4)_x(OH)_{2-x}$, following Winand (1961) or $Ca_{10-x-y}(HPO_4)_x(PO_4)_{6-x}(OH)_{2-x-2y}$, following Kühl & Nebergall (1963); where x ($0 \leq x \leq 2$) and y depend on different environmental and biological factors (Rollin-Martinet et al., 2013; Combes et al., 2016)] and, secondarily, calcium and phosphate salts (e.g., Eliott, 2002).

The bones are continuously altered over time, during the animal life, but especially after the death and the eventual burial of their skeletal system. Alterations occur at different scales: molecular loss, chemical substitution, elemental enrichment, crystallite reorganization, porosity and microstructural changes, which may lead to the destruction of the entire skeleton (Nielsen-Marsh & Hedges, 2000; Jaouen, 2018).

It is known that during the fossilization of bone tissues, the intra-bone porosity changes continuously with the degradation of biological material (Decrée et al., 2017) and several changes in hydroxylapatite mineral structure, composition, and lattice configuration may occur (Keenan et al., 2015; Keenan, 2016). These changes often depend on the depositional context, especially as regards to the

Fig. 1 - Localization of the site of La Polledrara di Cecanibbio (Latium, Italy).

characteristics (hydrological, geochemical, and mineralogical) of sediments within which the bones are buried, and circulating fluids (Pate et al., 1989; Nielsen-Marsh & Hedges, 2000; Berna et al., 2004; Trueman et al., 2004; Suarez & Passey, 2014; Suarez & Kohn, 2019).

Apatite crystals usually change (Berna et al., 2004; Trueman et al., 2004), and in the early stages of the fossilization process the carbonated hydroxylapatite is generally transformed in carbonated fluorapatite (Trueman et al., 2004; Thomas et al., 2007, 2011; Pasteris & Ding, 2009).

The fossilized bone tissue is often enriched in fluorine (F), iron (Fe), manganese (Mn), strontium (Sr), barium (Ba) and rare earth elements (REE) in different quantities, because of the exchange of Ca^{2+} cations with monovalent to hexavalent cations (Keenan et al., 2015, Owens et al., 2019). The addition of a proton to PO_4^{3-} and OH^- ions could made the apatite lattice suitable to the substitution with CO_3^{2-}. This process may lead to the substitution of OH^- by F^- and Cl^- ions, and to the formation of apatite phases enriched in fluoride and carbonate (Keenan et al., 2015 and references therein). The presence of these apatite phases in the fossilized bones provides further indications of fluids movement during diagenesis and both the permineralization and impregnation processes of the skeletal remains (Hubert et al., 1996). To scrutinize about the chemical characterization of fossilized bone tissues is, therefore, of pivotal importance for deciphering the past diagenetic processes and the alteration processes currently affecting the structure and chemical composition of the skeletal remains. This knowledge may give interesting hints for detecting the best strategies (including conservation and restoration protocols) to ensure their preservation over time (e.g., Mallouchou et al., 2018).

This research aims to disentangling between the chemical modifications undergone by the bone tissues of the fossil remains exposed *in situ* at the Middle Pleistocene site of La Polledrara di Cecanibbio (Roma) and the alterations generated in the period during which they remained exposed to the environmental agents on the depositional surface after being unearthed.

1.1. The Site: a synthetic overview

The site of La Polledrara di Cecanibbio (hereinafter LPC) is located about 22 kilometers north-west of Rome in the western sector of the Roman Basin, an area geologically characterised by a widespread volcanic and moderate tectonic activity and interested by the effect of Quaternary glacio-eustatic sea-level fluctuations (see Milli et al., 2011 and references therein) (Fig.1). The fossiliferous deposit was discovered in 1984. The excavation activity, developed between 1985 and 2013 with the financial support of the *Soprintendenza Speciale Archeologia Belle Arti e Paesaggio di Roma* (*SSABP-RM*), uncovered an area of about 1200 square meters mainly consisting in a riverbed, cut into a bank of compact volcaniclastic deposits (Anzidei et al., 2012; Castorina et al., 2015; Santucci et al., 2016). In 2000, a museum, covering an area of about 900 sq. m, was built thanks to a grant by *Ministero della cultura* with the aim to preserve the deposit and its archaeo-palaeontological record (Figs. 2-3).

The mammal remains are imbedded in fluvial and fluvio-palustrine deposits belonging to the informal lithostratigraphic units known in literature as Aurelia Formation (Conato et al., 1980). Such deposits constitute the filling of an incised valley formed during the sea-level fall following MIS 10. At LPC the fluvial and fluvio-palustrine sediments deposited during the vertical aggradation phase characterizing the sea-level rise that marks the transition to MIS 9 (Anzidei et al., 2012; Santucci et al., 2016; Cerilli & Fiore, 2018). Pereira et al. (2017) recently refined the $^{40}Ar/^{39}Ar$ and ESR/U-series age for la Polledrara fossiliferous layers to 325 ± 6 ka confirming the chronology already suggested by Anzidei et al. (2012).

The fauna, consisting in more than 20,000 skeletal

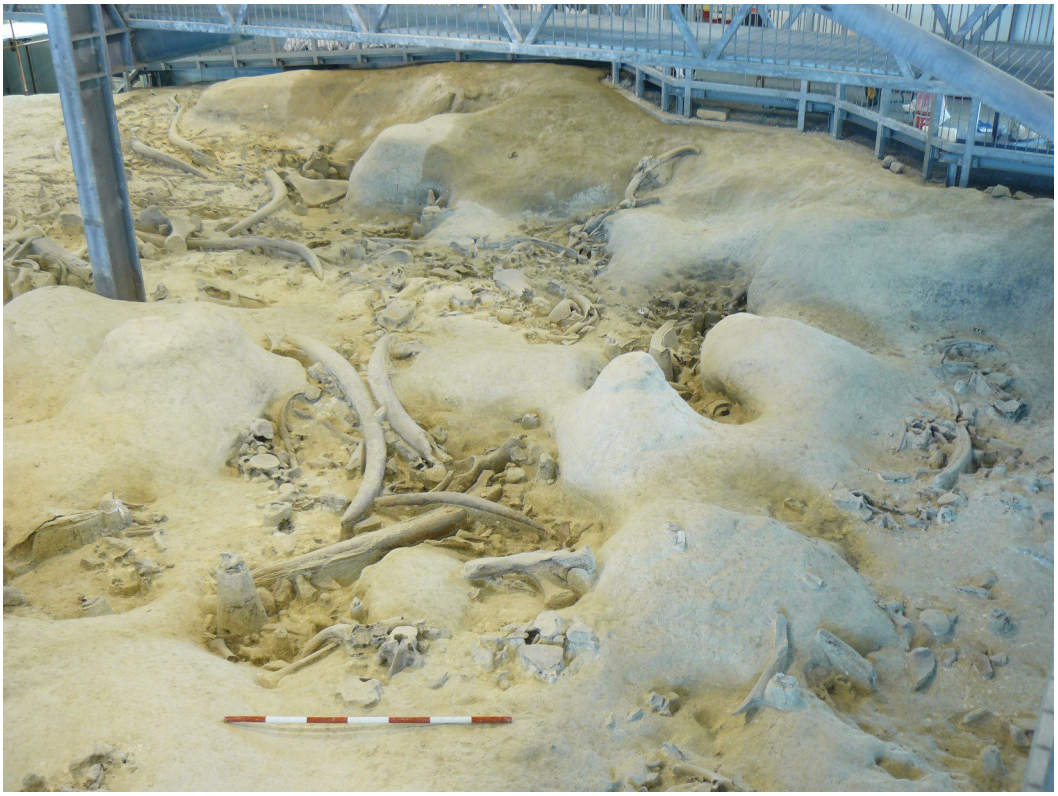

Fig. 2 - Overview on the museum's showcase of the site, seen by NW (SSABAP-RM archive).

Fig. 3 - Overview on the museum's showcase of the site, seen by SW (SSABAP-RM archive).

Samples	Description	Investigated portion	Investigation techniques
PdC 1	*P. antiquus* diaphysis fragment	Cortical – exposed surface	SEM-EDS
PdC 2	*P. antiquus* bone fragment	Inner portion	SEM-EDS
PdC 3	*B. primigenius* horn fragment	Cortical – exposed surface	SEM-EDS
PdC 4	Unspecified bone fragment.	Powder of cortical – exposed surface	XRD
PdC 5	Unspecified bone fragment	Powder - inner portion	XRD
PdC 6	*P. antiquus* skull fragment	Cortical – exposed surface	Raman
PdC 7a	*P. antiquus* rib fragment	From exposed surface to inner portion	SEM-EDS
PdC 7b	*P. antiquus* rib fragment	From exposed surface to inner portion	Raman
PdC 8	Unspecified bone fragment	Inner portion	Raman
PdC 9	*P. antiquus* long bone fragment	Cortical – exposed surface	SEM-EDS
PdC10	Sedimentary nodule	Inner	SEM-EDS

Tab. 1 - Selected fossil bone samples collected *in situ* and investigation techniques used.

remains, is dominated by large mammals (Anzidei et al., 2012), being *Bos primigenius* and *Palaeoloxodon antiquus* the most abundant species, followed by *Cervus elaphus*. The presence of *Sus scrofa*, *Stephanorhinus* cf. *S. hemitoechus*, *Bubalus murrensis*, *Equus ferus*, *Canis lupus*, *Vulpes vulpes*, *Meles meles*, *Felis silvestris*, *Macaca sylvanus*, *Leporidae* gen. spec.indet., is documented by few remains. The remains of small mammal and birds are, however, numerous. Both murids (*Apodemus sylvaticus*, *Iberomys* cf. *I. breccensis*) and arvicolids (*Pliomys* cf. *P. episcopalis*, *Arvicola* sp.) are present, and in the rich avifauna, Anseriformes species prevail (Monica Gala personal communication). The herpethofauna is still under study.

Although the lack of pollen and plant fossil remains prevents any compelling reconstruction of the vegetation cover, a few hints are provided by the ecological structure of the fauna and dental microwear and isotope analysis. The landscape at LPC was probably characterized by a dense arboreal cover interspersed with open spaces in conditions of moderately humid and temperate/warm-temperate climate (Filippi et al., 2001; Palombo et al., 2005).

The temporary attendance at the site of hominin groups is documented by the presence of hundreds of artefacts on flint pebbles and flakes (denticulates, notches, side- and end-scrapers, multiple use tools), by some tools made on elephant bones, and by several bones intentionally fractured for marrow extraction (Anzidei & Cerilli, 2001). LPC likely represented an attractive area as a source of food and raw material, for the hunter-gatherer groups that frequented the surrounding territory (Anzidei et al., 2015). The presence of muddy, palustrine zones near to the river banks occasionally acted as traps for elephants as documented by the presence of two skeletons with zeugopodia and autopodia still in anatomical connection and in life position. A third skeleton, lying with limb bones in anatomical connection gently bent on its left side on the riverbank, is surrounded on both sides by hundreds of lithic implements, produced in situ and used for cutting soft tissue (Santucci et al., 2016). Available evidence indicates that at LPC human group scavenged an elephant carcass, which died from natural causes, probably after sliding on the mud-covered bank at the edge of a palustrine zone, and having been trapped in the muddy sediments of a puddle. The butchery activity on elephant carcass is also documented by the presence of cut marks on a bone fragments (Palombo & Cerilli, in press and references therein).

The single human remain found to date is a deciduous second upper molar of a child, 5-10 years old (Anzidei et al., 2012). The tooth has been tentatively ascribed to *Homo heidelbergensis*, a species recorded in Italy, among others, at the Middle Pleistocene site of Ceprano (Frosinone) (Manzi et al., 2010; Manzi, 2016; Bidditu et al., 2020; Buzi et al., 2021 and references therein) and to which some scholars ascribed the rich population from the well-known Spanish site of Sima de los Huesos (Atapuerca, Northen Spain), regarded by others as belonging to the Neanderthal lineage (e.g Stringer, 2012; Buck & Stringer, 2014; Manzi, 2016; Hanagraef et al., 2018; Roksandic et al., 2018, 2019).

2. MATERIAL AND METHODS

2.1. Material

The material selected, treated and prepared for the multidisciplinary analysis consists of eleven samples of one sedimentary nodule and 10 bone fragments collected from the surface of the riverbed (Tab. 1). The samples were selected taking into account the time of the exposure: i.e. all samples belong to fossil bones or fragments exposed for more than 10 years at the site. The exposed surface of the bones, and both the cortical and the inner portion of the samples were analyzed by means of the following techniques.

2.1. Methods

2.2.1. Indoor environmental parameters

The knowledge of the indoor environmental parameters is of fundamental importance for understanding the ongoing alteration processes affecting the fossil bones and preserving them over time.

We have hourly recorded the main environmental parameters [Temperature (°C), Relative Humidity (%) and Dew Point (°C)] between February and April 2015 for a period of 60 days, and for 25 days in September 2015. This enables us to estimate the trend of the environmental parameters inside the museum during two seasons (late winter / early spring and the late summer). The measures have been taken with three data loggers (Lascar electron-

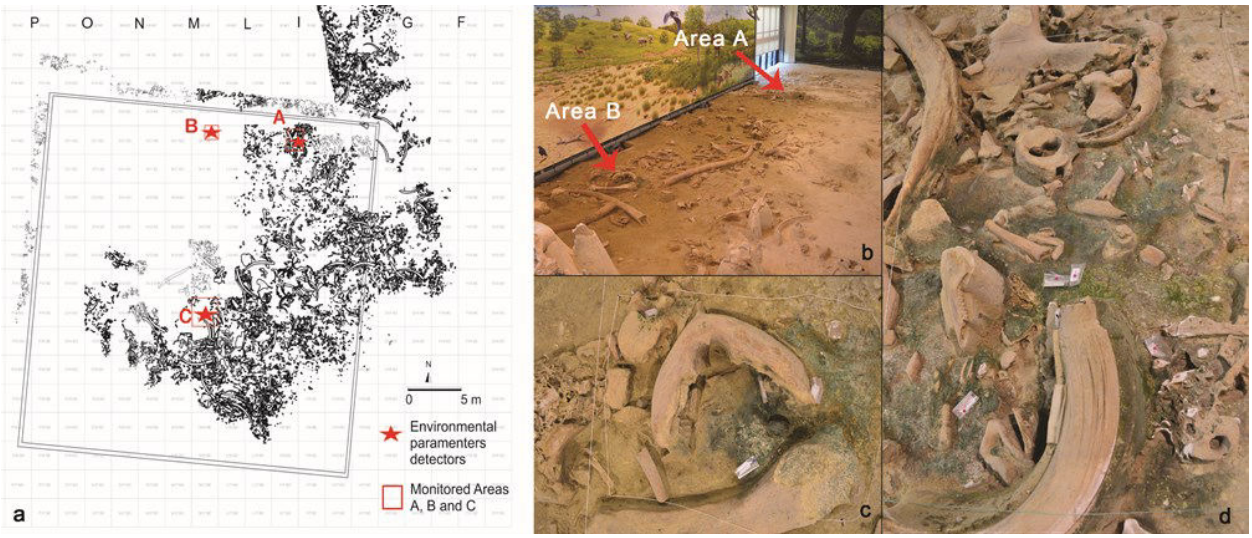

Fig. 4 - a) Plan of the excavation with the localization of monitored areas; double square represents the museum walls. b) A panoramic view of the northern sector of the exposed paleosurface; the red arrows indicate the monitored areas A and B. c) Monitored area B: view of the exposed and sampled bones. d) Monitored area A: view of the exposed and sampled bones.

ics, EL-USB-1HDT-250, Thermosense, UK) positioned in three different zones (A-B-C) of the paleo-riverbed. The selected areas are located along the northern wall (A and B), and in a central part (area C) of the museum (square M14) (Fig. 4). Information about the humidity and temperature trends throughout time has been inferred by means of the average daily collected data.

2.2.2. X-ray Diffraction analysis (XRD)

The XRD allows defining the main mineral phases composing the fossil bones. The analysis was carried out on a sample obtained 1 cm below the exposed surface and prepared by grinding the bone in a mortar to obtain a fine powder. Two samples (PdC 4 and PdC 5) were Powered-XRD analysed in the aim of defining the main mineralogical phases of the fossil bones. PdC4 and PdC5 consist respectively of a thin exfoliated portion and a bone carrot extracted by means of a cup with a diameter of 2.5 cm, both obtained from large mammal (bovid or elephant) bone fragments. In PdC5 only the innermost portion was preserved because the coring damaged the cortical portion that was not analysed.

The analysis was conducted at X-ray Powered diffraction laboratory of *Dipartimento di Scienze della Terra, SAPIENZA Università di Roma* by means of the automatic diffractometer SIEMENS/Bruker D-5000 XRD at 40 kV and 30 mA with an acquisition step of 2.0 seconds each 0.2 degrees. The interpretation and the identification of the mineral phases were based on the database of XPower12 Ver.01.02.

2.2.3. Raman Spectroscopy analysis

Raman spectroscopy analysis (SERS: Confocal and surface-enhanced Raman spectroscopy, and TERS: Tip-enhanced Raman spectroscopy) consists of powerful techniques for molecular characterization, and it is a very promising method for studying complex biological systems (Ferraro et al., 2003; Zong et al., 2018; Kumar et al., 2019). Qualitative and quantitative analyses constitute two of the most important aspects of SERS application in analytical science (Zong et al, 2018), and represent a compelling integration to other analytical methodologies.

The measurements were carried out with a Horiba™ LabRAM HR Evolution confocal Raman microscope in back scattering geometry. Samples were excited by the 632.8 nm radiation of a He-Ne laser with 30 mW output power (15 mW on the sample). The detected peaks have been compared with RRUFF™ Project database (rruff.info) and elaborated with ORIGIN software by OriginLab©. The technique does not require a specific preparation of the samples.

The Raman Spettroscopy was applied on samples PdC 6, 7b and 8 in order to integrate the XRD dates by determining the mineralogical composition over a micrometric scale, and ascertaining the ionic substitutions in the original bone mineral structure during the burial. PdC6 is a *P. antiquus* maxillary fragment. PdC7b is a transverse section of a *P. antiquus* rib, obtained cutting the bone with a saw. PdC7b was analysed by means of a spectroscopic map carried out from the exposed surface towards the lymphatic canal of the osteon. PdC8 is an exfoliated portion sampled from a long bone fragment of an unidentified large mammal.

2.2.4. SEM-EDS analysis

Scanning Electron Microscopy with Energy Dispersive X-ray Spectrometry (SEM/EDS) is an elemental microanalysis technique widely applied in physical and biological sciences, engineering, technology, and forensic investigations (Goldstein et al., 2018).

At LPC, SEM- EDS analysis was carried out on samples PdC 1, PdC 2, PdC 3 PdC 7a, PdC 9 and PdC10 for providing the elemental composition of a selected area of the bone sample and obtaining, thanks to high resolution images, information about the structure of bone tissue and the general physical characteristics. The samples were collected from two long bone fragments (PdC 1, PdC 9), rib fragment (PdC 7a), and an unspecified fragment (PdC

	Temperature (°C)			Relative Humidity (%)			Dew Point (°C)		
	Min	Mean	Max	Min	Mean	Max	Min	Mean	Max
Area A									
feb	8.5	11.0	13.5	80.0	96.0	101.5	6.9	10.3	13.0
mar	7.5	11.7	16.0	90.5	100.4	104.5	6.3	11.8	16.3
apr	9.0	13.1	17.0	91.5	100.0	104.0	8.4	13.1	17.0
sept	17.5	21.2	26.0	84.5	95.8	100.0	16.8	20.4	24.7
Area B									
feb	8.5	10.6	12.5	80.5	95.6	101.0	6.5	9.9	12.4
mar	7.0	11.4	15.5	90.0	100.0	104.0	5.6	11.4	15.8
apr	8.5	12.7	16.0	91.5	99.9	103.5	7.7	12.7	16.2
sept	17.5	20.7	25.5	86	97.7	101.0	17.2	20.3	24.4
Area C									
feb	9.0	11.4	14.0	77.5	92.2	97.0	7.1	10.2	13.3
mar	8.0	12.3	16.5	89.0	96.3	100.5	6.5	11.7	16.3
apr	9.5	13.7	17.5	90.0	96.1	100.0	8.4	13.1	17.0
sept	18.5	21.8	26.5	82.5	89.1	93.0	16.3	19.9	24.5

Tab. 2 - Environmental parameters monitored at the site during the months of February, March, April and September 2015 in the areas A, B and C. Min, Mean and Max values of the Temperature (T °C), Relative Humidity (RH %) and Dew Point (DP ° C) are reported.

2) of *P. antiquus*, from a horn-core fragment of *B. primigenius* (PdC 3), and from a sedimentary nodule (PdC10) (Tab 1). The samples were obtained by extracting small fragments of the bone cortical portion by means of a small chisel and a hammer, except for PdC 7a from which a thin cross-section was obtained. The analyses were conducted mainly on the exposed surface of the bone, except for PdC2 and PdC7a where the inner portion was analyzed.

The bone samples were fixed on stabs of 1 cm diameter and coated with a thin layer of graphite or gold and analyzed in a vacuum chamber. The acquisitions were conducted in low vacuum with different parameters of pressure, magnification and work distance, depending on the samples. The samples were analyzed at the *Laboratory of Electron Microscopy and Micro-analyses of the Dipartimento di Scienze della Terra, SAPIENZA Università di Roma*, by means of a scanning electron microscope Thermo Fisher Scientific™ FEI Quanta™ 400.

3. RESULTS

3.1. Indoor environmental parameters

The values of temperature (°C) and relative humidity (%) measured during the end of winter to the beginning of spring and the late summer highlight a similar trend of the average temperature in the three monitored areas (A, B, C), though the daily values change considerably from an area to another. The highest and lowest temperatures were recorded in the area C (located in central part of the museum) and B (located near the northern wall of the museum) respectively. In the area A (located close to the windows is exposed to the sun in the first part of the day) the values of temperature are halfway. As expected, the temperatures recorded during the day and the night differ considerably.

In the area A, the average temperature varies from 11°C in February to 21.2°C in September, with a minimum and maximum value of 8.5°C and 13.5°C in February and 17.5°C and 26°C in September. In the area B, the average temperature varies from 10.6°C in February to 20.7°C in September, with a minimum and maximum value of 8.5°C and 12.5°C in February and 17.5°C and 25.5°C in September. In the area C, the average temperature varies from 11.4°C in February to 21.8°C in September, with a minimum and maximum value of between 9°C and 14°C in February and 18.5°C and 26.5°C in September.

Conversely, the average daily relative humidity does not substantially differ in the areas A and B, while the area C is drier.

In the area A, the average relative humidity varies from 96% in February to 95.8%° in September, with a minimum and maximum value of 80% and 100% in February and of 84.5% and 100% in September. In the area B, the average relative humidity varies from 95.6% in February to 97.7% in September, with a minimum and maximum value of 80.5% and 100% in February and 86% and 100% in September. In the area C, the average relative humidity varies from 92.2% in February to 89.1% in September, with a minimum and maximum value of 77.5% and 97% in February and 82.5% and 93% in September (Tab 2).

The higher relative humidity in the area A and B likely depends on their temperature variations, which often intercept the dew point line. As a result, the air approaches the saturation point and the water availability increase. In the area C, where the temperatures are always higher than the dew point, the availability of water is virtually nothing (Fig. 5).

3.2. Mineralogical and chemical composition

3.2.1. XRD analysis

The XRD analysis enables us to identify the main mineral phases characterizing the samples PdC4 and PdC5. In PdC4, three mineral phases have been identified: Fluoroapatite ($Ca_{10}(PO_4)_6F_2$ according to Leroy and Bres, 2001), Gypsum-Calcium ($CaSO_4$) and a sorosilicate mainly composed of Ba, which respectively correspond to three peaks of decreasing intensity in the spectrum (Fig. 6a). The XRD spectrum of the samples PdC5 is characterized by two main mineral phases identified as Fluorapatite and Barite ($BaSO_4$) (Fig. 6b).

3.2.2. Raman Spectroscopy

As regards Raman Spectroscopy, two different acquisition point (Pt1 and Pt2) were detected on sample PdC8 showing a main frequency of the PO_4^{3-} site at 960 cm^{-1} as typical of apatite group $Ca_5(PO_4)_3$[F, OH, Cl]. The Raman spectrum of the Pt2 shows another spectral structure corresponding to 600 cm^{-1} referred to magnesioferrite mineral. Moreover, the peaks of 960 cm^{-1} are lightly blue-shifted reaching a frequency of 964,0 +- 0,2 cm^{-1} and the FWHM (Full Width at Half Maximum Height) at 10,5 + -0,2 cm^{-1}. According to RRUFF™ Project database (rruff.info) it is reliable to attribute the peaks to the fluoroapatite, confirming as detected by XRD. The colored thermal scale obtained by spectroscopic map carried out on

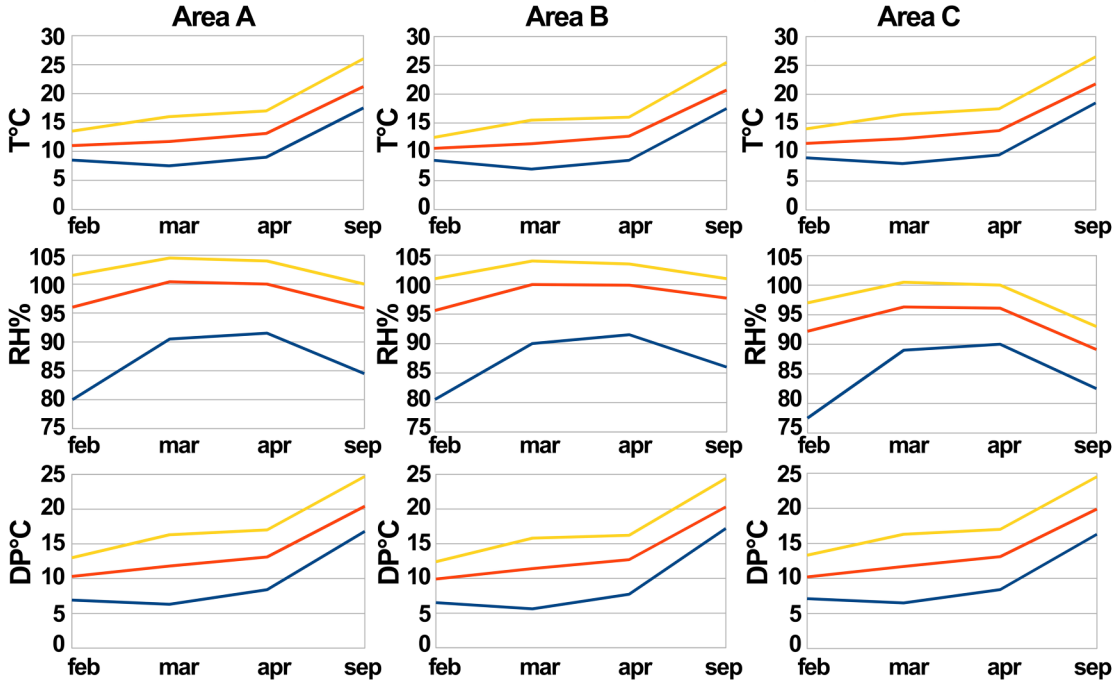

Fig. 5 - Trend of daily temperature (T °C), relative humidity (RH %) and dew point (DP °C) - maximum (yellow line), medium (red line), and minimum (blue line), monitored in areas A, B and C during the months of February, March, April and September 2015.

the sample PdC7b shows a uniform intensity signal of the peak at 960 cm-1 in correspondence of osteon.

3.2.3. SEM-EDS analysis

The results obtained by SEM EDS analysis highlight a permineralization of sulfates crystals impregnating the bone tissue and sometimes incrusting the bone surface. In the sample PdC1, the external surface of the analyzed fossil bones rough, compact and, locally slightly fractured. The elemental peaks detected by EDS, revealed a main composition in phosphorus (P) and calcium (Ca), as it typically occurs in bone apatite (Fig. 7). Other accessory peaks such as silicon (Si), aluminum (Al), magnesium (Mg), and fluorine (F) have also been detected. In sample PdC3 and PdC9, the surface of the bone is characterized by the presence of crystals composed mainly by sulphur

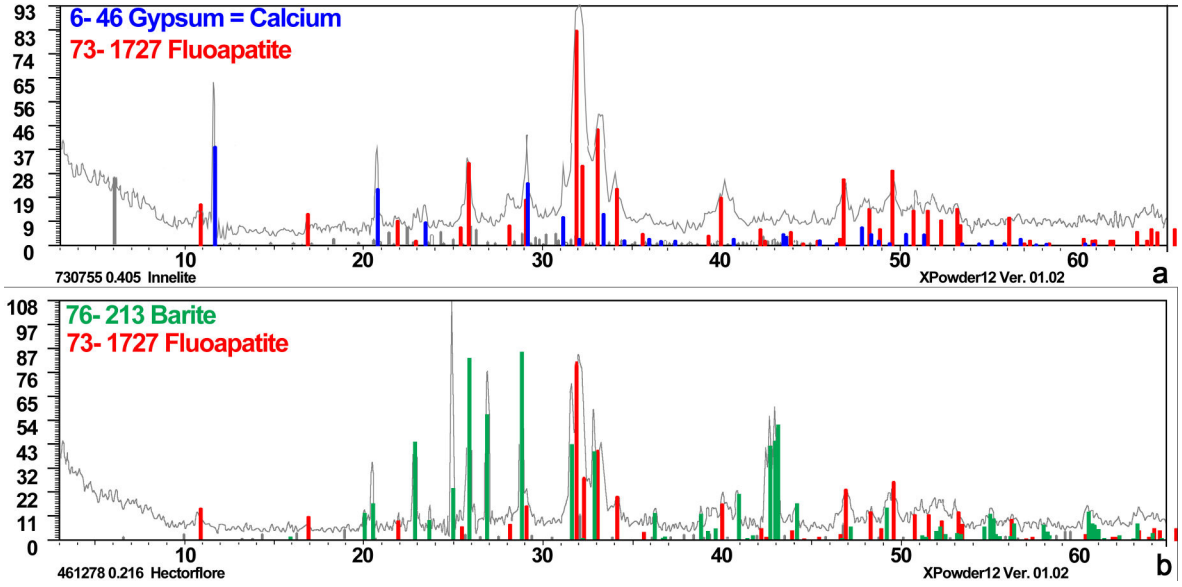

Fig. 6 - a) X-Ray Powered diffraction spectrum of the sample PdC4, two main peaks have been recognized: Fluoroapatite (red), and Gypsum (blue); b) X-Ray Powered diffraction spectrum of the sample PdC5 where two main peaks have been recognized: Barite (green) and Fluoroapatite (red).

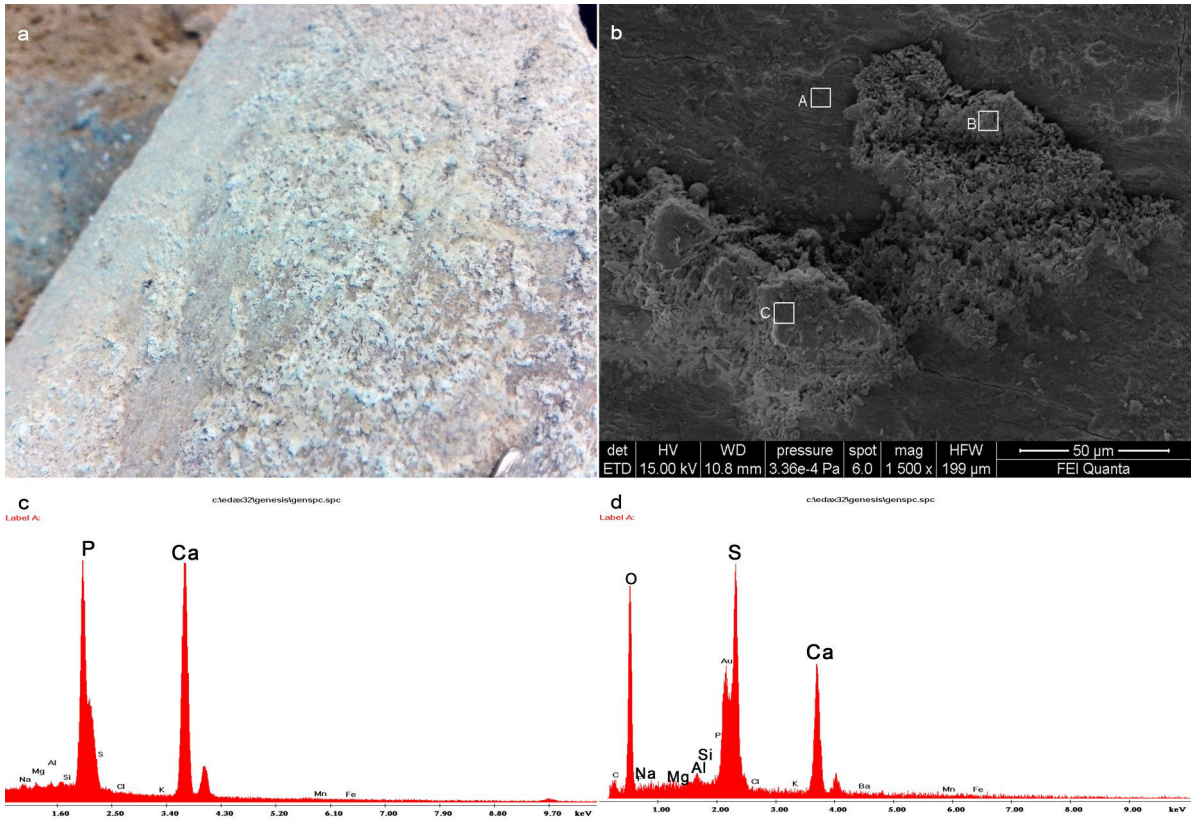

Fig. 7 - a) Gypsum efflorescence on *P. antiquus* diaphysis exposed *in situ* where the sample PdC1 was collected from; b) SEM image at 1500 magnification of sample PdC1, the squares A, B and C represent the point where the elemental analyses with EDS has been conducted; c) the EDS spot at the point A, corresponding to the bone surface, is characterized by typical peaks of the Apatite with elemental composition in Calcium (C) and Phosphorus (P); d) the EDS spot at the points B and C, corresponding to whitish efflorescence visible on the exposed bone, where the main elemental peaks are Sulphur (S) and Calcium (Ca).

(S) and calcium (Ca) in addition to the P and Ca peaks (Fig. 8).

In the sections (samples PdC2 and PdC7a), observed transversally from the cortical surface of the bone toward the inner portion, a compact structure of the bone with some fractures has been observed and the osteons and lymphatic canals have been recognized. In PdC2, some canals are not empty but filled with several prismatic and sometime tabular crystals (Fig. 9). In PdC7a, most of the Haversian canal situated in the portion of the sample corresponding to the bone part lying on the riverbed, and the main bone fractures are filled with tabular crystals (Fig. 10a). In both samples the crystals grow usually in a definite and oriented direction and are composed by barium (Ba) and sulphur (S) (Figs. 9d and 10de).

In all EDS spots, the Ba shows three peaks (α, β and γ) indicating the presence of its complete phase (Figs 9e and 10f). The association of the elements we have found suggests the presence of barium sulphate or barite ($BaSO_4$).

In the sedimentary nodule PdC10, the internal part is characterized by euhedral tabular and elongated crystals of Barite (Fig. 11).

4. DISCUSSION

4.1. Indoor environmental parameters

The alteration processes affecting the fossil bones at LPC (especially the dissolution and re-precipitation of sulphates) mainly depend on the notable seasonal changes and intense thermal daily excursion of the indoor environmental parameters (temperature and humidity).

The humidity at the site is mainly related to the water that during the rainy period, due to capillarity action in the porous volcanic sediments, makes the paleo-riverbed moist. On the one hand, the enriched water availability on both sediment and bone surfaces activates the crystallization-dissolution cycles of salts, gypsum in particular. On the other hand, during drought period, the increasing in dryness could cause mechanical damages, sometimes confused with modifications caused by diagenetic process. Salts precipitation happened due to thermo-hygrometric factors provokes, indeed, to fossil bones a number of damages (even on a very small scale) such as fractures, crumbling of the exposed surface, erosion and disintegration (Benavente et al., 2011).

Therefore, it is probable that the gypsum detected in the bones at LPC is due to its facility of precipitation in the

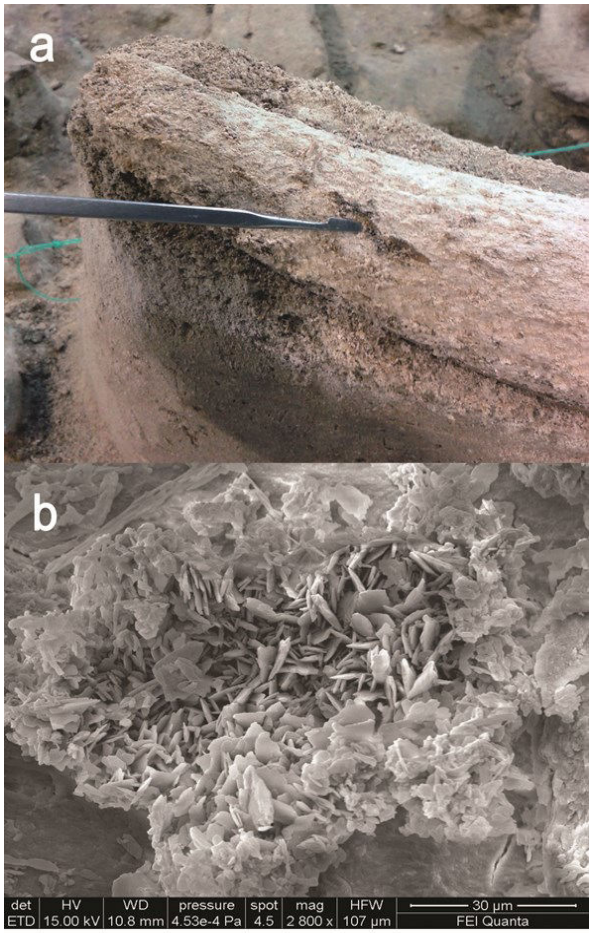

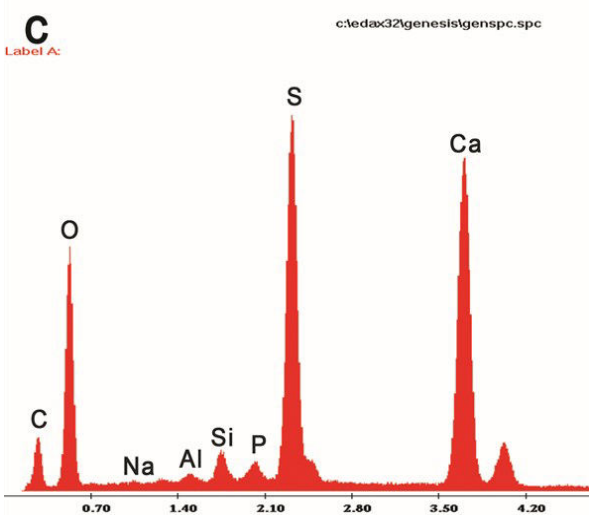

Fig. 8 - a) *Bos primigenius* horn exposed *in situ* where the sample PdC3 was collected from, the fossil is characterized by salts efflorescence causing exfoliation and disintegration; b) SEM image at the 2800 magnification of the sample PdC3, the crystal clusters are characterized by rose-like shape as typical of gypsum crystals; c) the EDS elemental spot showing the composition of the crystals in Ca and S ascribed to Calcium Sulphate (gypsum).

fractures of diagenetic origin and induced by cracks derived from dissolution-recrystallization cycles. It could be also hypothesized that the precipitation of barium salt (barite) inside the bone fractures and cavities (though occurring at a different time and with a different pace) may be triggered by the alternating environmental conditions at the site.

The environmental conditions recorded at LPC also cause the growth of photosynthetic biofilm both on sediments and the fossil bone surface, especially where there is water availability, producing at first aesthetic detrimental effects. Marano et al. (2016) documented the presence of a number of associated microorganisms such as algae, fungi and mosses. In particular the authors focused the attention on cyanobacteria belonging to the genus *Leptolyngbya*, which colonizes and grows on the exposed surface of the fossil bones at LPC. The endolitic power of the representatives this genus have been documented as regards to the deterioration of marble, façade, limestone monuments and Roman catacombs (Tomaselli et al., 2000; Miller et al., 2009; Bruno & Valle, 2017; Gallego-Cartagena et al., 2020), and can be also hypothesized for the fossils of LPC. The chemical composition, the roughness of the surface, the porosity and the texture of the substrata are discriminating factors that control the bioreceptivity of the material (Korkang & Savran, 2015). The elements composing the bone substrata are mainly P and Ca, but also other elements, such as Potassium, Sulphur, Iron and Magnesium have been detected by EDS analysis. These are the essential trophic elements for the growth of cyanobacteria and algae. Moreover the presence of gypsum as component of saline efflorescence could increase the trophic system and can be used by cyanobacteria as sulfate source (Vijayakumar, 2014), increasing the damage risk for La Polledrara bones.

4.2. Mineralogical and chemical composition

The identification of mineralogical and chemical composition of fossil bones has a pivotal importance for proper understanding of the biostratinomic processes and the diagenetic mechanisms leading to the preservation of vertebrate remains in their deposition context, (Trueman et al., 2004; McLaughlin & Lendev, 2011; Piga et al., 2011 and reference therein; Thomas et al., 2011). Similarly, it is crucial to ascertain to which extend environmental physical and biotic factor may affect the status of fossil bones if they are displayed *in situ*, on the surface of the sediment they were retrieved from. Knowing past and ongoing processes of bone modifications enable planning the correct procedures to avoid and limit any potential deterioration process. The deterioration processes may be caused by several factors, most related to the environmental parameters, such as temperature and humidity, and their instability. Available evidence confirms, indeed, that water and light are among the main factors causing deterioration of palaeontological and archaeological material exposed to environmental agents (Caneva & Ceschin, 2007).

Several authors consider the process of fluoritisation of the Hydroxylapatite (i.e. the replacement of OH- ions by F- ion), directly related to the neighboring environment

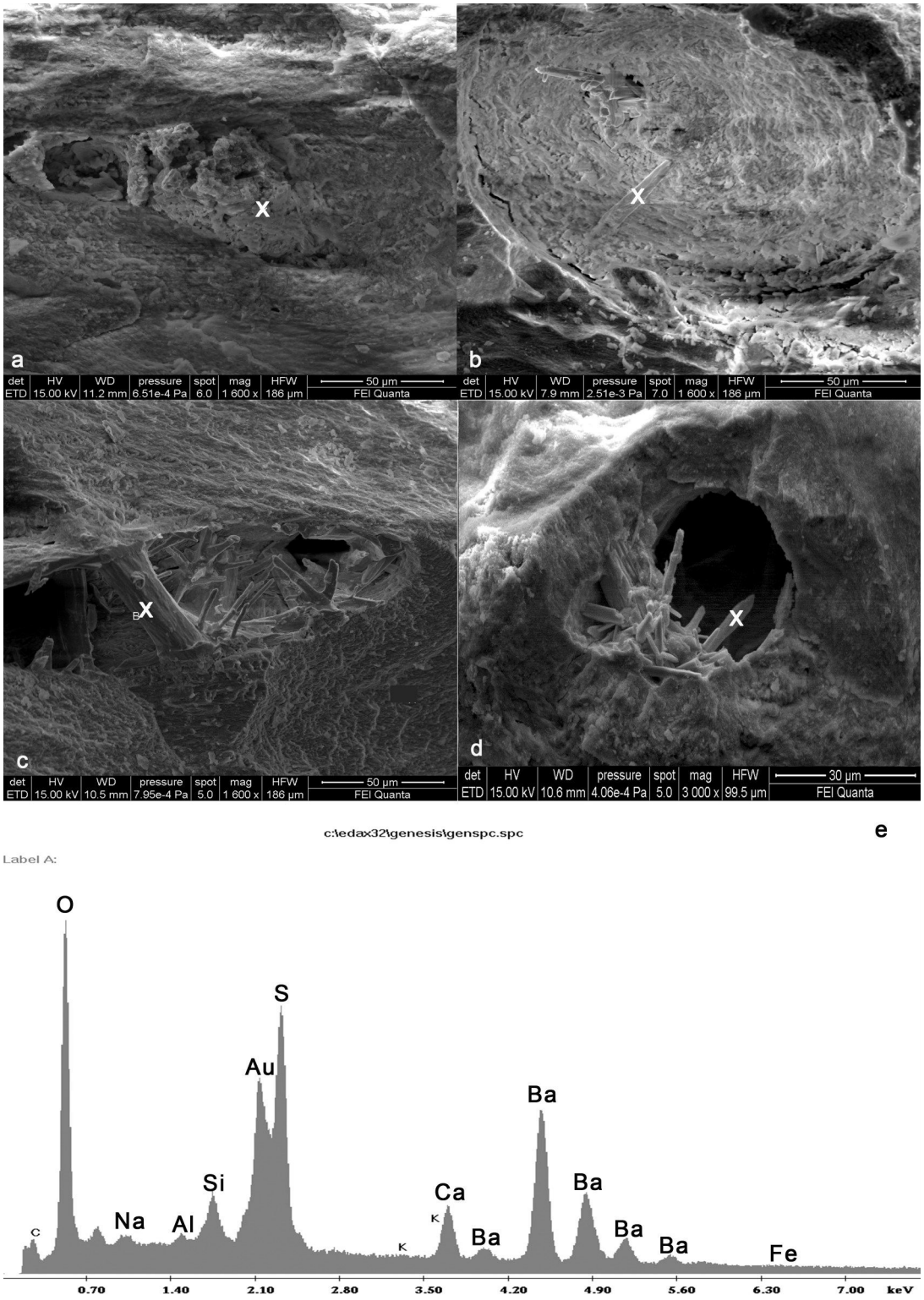

Fig. 9 -SEM-EDS images of Barium Sulphate crystals found during the observation of the cortical portion of the fossils (PdC2), X corresponds to detected points: a, b and c) SEM images at 1600 magnification showing fractures and channels filled with Barite euhedral tabular crystals; d) SEM image at 3000 magnification with Barite crystals growing in a channel; e) EDS spot conducted on crystals showing all peak of Ba and S.

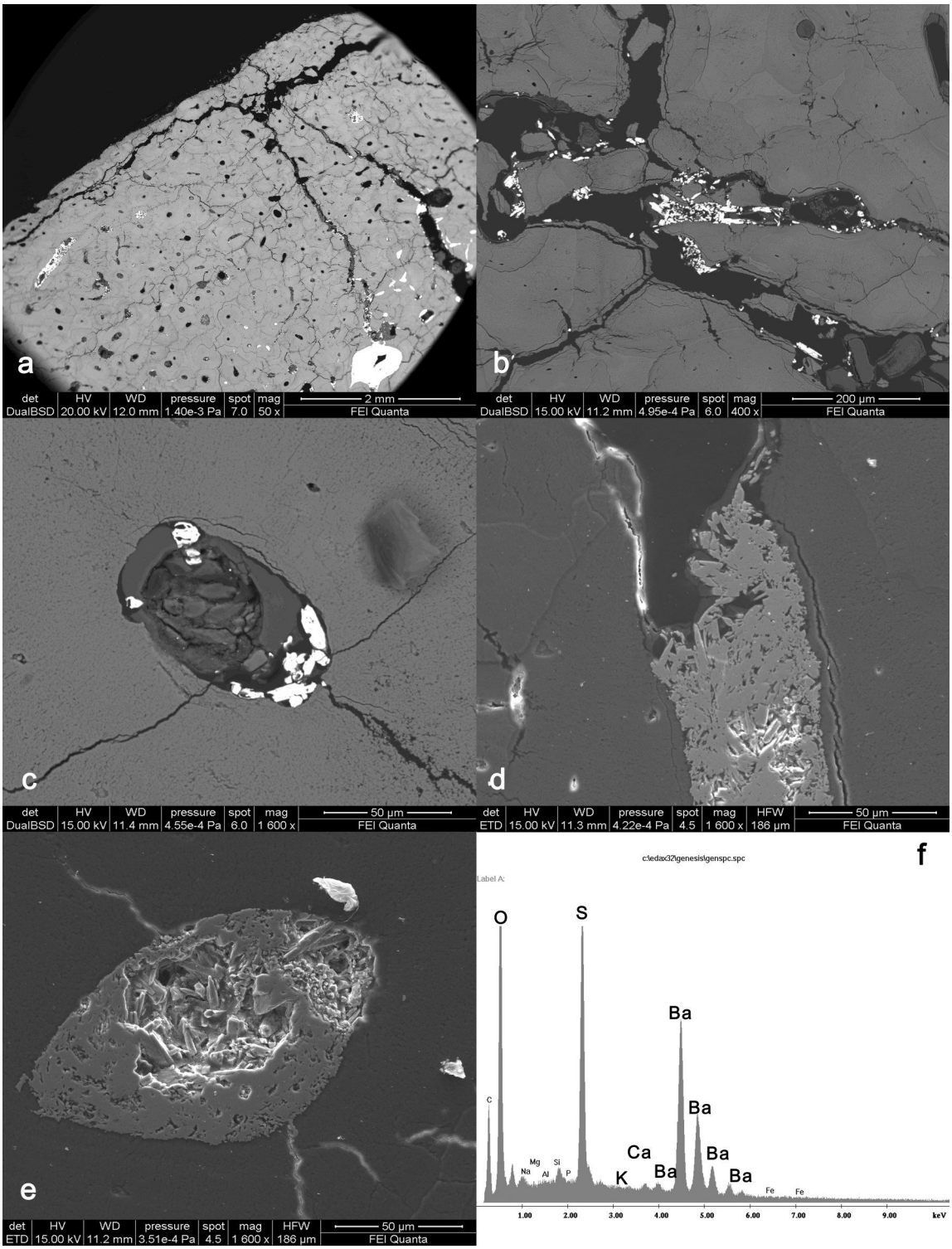

Fig. 10 - SEM-EDS images of the thin transversal section (PdC7a) obtained from an elephant rib. The section is oriented: the upper part corresponds to the exposed surface while the lower portion lay on the paleo riverbed. a) the section at 50 magnifications shows the internal structure with the osteons and Haversian canals, a series of main fractures are visible running from the top to the bottom of the sample and transversally specially in uppermost portion, micro fractures are also present on entire surface of the sample; b, c) some of the biggest fractures and some osteons at the bottom of the sample appear filled with crystal that give a white fluorescence; d) the big fracture crossing the whole section where euhedral crystals are growing upward; f) EDS spot detected on crystals filling the fractures and Haversian channels showing all peaks of Ba and S.

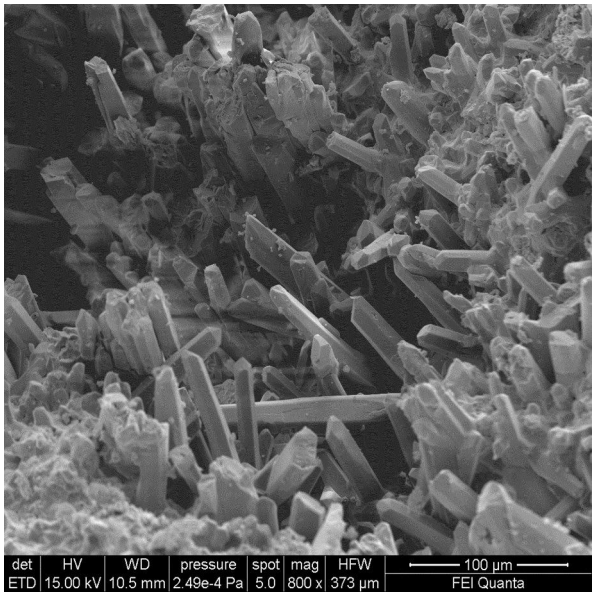

Fig. 11 - SEM images at 800 magnification of the inner portion of sedimentary nodule (PdC10) characterized by elongated, tabular and oriented crystals. Ba and S characterize their elemental composition.

characteristics (Leroy & Bress, 2001; Thomas et al., 2007, 2011) and the most frequent process of substitution undergone by the biogenic apatite (Piga et al., 2009, 2011).

Arnoldus & Anzidei (1993) and Arnoldus et al. (2001), detecting the presence of the gypsum ($CaSO_4$) and barite ($BaSO_4$) only in sediments, hypothesized that the process of fossilization of the LPC bones may have triggered by their indirect contact with ashes and fluorine-containing water.

The presence at LPC of fluorine in the fossil bones and in a number of the abundant centimetric nodules present in sediments filling the paleo-riverbed (particularly near the river bottom) is in agreement with the high content of Ba detected as trace element in the uppermost sediments of the local stratigraphic section (Castorina et al., 2015). A high concentration of Ba forming barium sulfate minerals has been reported in some fluorine deposits cropping out in Northern Latium, but its origin and genesis are still a matter of debate (Matteucci, 1976; Di Sabatino et al., 1979; De Rita et al., 2012). Several deposits of barite and other sulfates such as Celestine ($SrSO_4$) have been recognized and described in territories surrounding the LPC area (Barbieri & Masi, 1978). Mastrangelo (1976), for instance, described some fluoride deposits enriched in barite minerals at Valle Santa, a locality few kilometers north to LPC. The same deposits are correlated by Arnoldus & Anzidei (1993) with the fluoride whitish layers outcropping near La Polledrara fossiliferous deposit.

Trueman et al. (2004) detected the presence of barite as the second most abundant authigenic mineral, formed in situ in response to the geochemical process in several recent bones exposed during a time of 26 years in the tropical savannah environment of Amboseli National Park. The presence of barite crystals concentrated in the most external osteon cavities suggests a fast precipitation of the mineral in response to the circulation features of the ground water and the elements dissolved in it. Scrutinizing processes leading to the presence of Ba may provide some clues about the hydrochemistry characteristics of a terrestrial environment during the animal life (Brügmann et al., 2012; Hanor, 2000). Merk et al. (2017), for instance, aiming at scrutinizing the biomineralization processes in the plant kingdom, experimented how the $BaSO_4$ organizes the crystals in a wood structure. The authors obtained an oriented growth of $BaSO_4$ crystals confined in the complex and highly directional cell architecture of wood, highlighting a prevalent and fast crystallization of $BaSO_4$ at different hierarchical levels in the cavities.

At LPC, the presence of Ba forming barite crystals in the bone tissue cavities provides some hints about biostratinomic processes and the hydrochemistry characterizing the environment during the burial and fossilization phases. The presence of barium sulfate crystals, oriented in the osteonic (haversian) canal and in the main fractures, which were produced by weathering and transport before the burial, indicates that the circulation of ground waters enriched in high contents of ions Ba^+ and SO_4^{2-} and F favored both the precipitation of barite mineral in the cavities of bone tissue and fractures and the hydroxlyapatite fluoritization process skeletal remains after their deposition and burial process.

Arnoldus & Anzidei (2001) reported the presence of some large imprints of radial gypsum crystals in La Polledrara fossiliferous sediments. They were likely originated by the chemical interaction between the bone calcium and the sulphur contained in the circulating fluids or gasses. A large amount of carbonates and sulfates, accompanied by other elements, is present both in the deep hydrothermal reservoir and in the shallower water reservoir of the Sabatini Volcanic District (Cinti et al., 2017, 2019, and reference therein). Therefore, it is rationale to suppose that both the calcium present in the bones and mainly the Ca^+ ions typically circulating in groundwater of the Sabatini Volcanic District supplied the Ca^+ needed for the gypsum precipitation. Some gypsum crystals have also been detected on the surface of the fossil bones at LPC. Their “rose-like” shape indicates a very fast precipitation, comparable with that of the whitish efflorescence that affects archaeological building stones.

The gypsum efflorescence have been acknowledged to be the principal salt sulphate causing deterioration on cultural heritage (mortar, paintings, facades, hypogea environment, and building stones in general) (Rodriguez-Navarro & Doehne, 1999; Bugini et al., 2000; Albertano et al., 2003; Rijniers et al., 2005; Cardell et al., 2008; Benavente et al., 2011; Lopez-Arce et al., 2011; Barca et al., 2014 and references therein; Zammit et al., 2011) and triggering the developing of microorganisms (Marano et al, 2016; Lepinay et al., 2018, and reference therein; Marano unpublished data).

The high solubility of this salt and the facility of expansion upon its re-precipitation inside the bone structures constitute the main cause of deterioration. Since the crystallization of secondary minerals such as gypsum crystals is strictly related to environmental condition and in particular to the humidity and water availability, a monitoring of the environmental conditions is of crucial important for the preservation of fossil bones whatever they are kept or displayed.

5. CONCLUSION

The identification of befitting conservation strategies is of crucial relevance especially in the case of skeletal remains preserved *in situ* and possibly exposed to the aggression of biotic and abiotic agents, such as humidity, temperature, sunshine, possible aggression of biological agents, particularly the growth of biofilms. The musealized portion of the La Polledrara di Cecanibbio fossiliferous deposit, one of the richest in *P. antiquus* remains and the most fascinating in Italy, offered a pivotal case study for deconstructing pattern and processes of fossil bones deterioration and inferring compelling protection actions.

Results obtained by this study highlight the particular importance the determination of the indoor environmental parameters has for properly understanding the alteration processes in progress and disentangling the past processes related to biostratinomy and diagenesis.

Fluoritization was the main process occurring during the diagenetic modification of the bone remains at LPC that favored the fossilization. The presence of oriented Barite crystals, detected in the main fracture and in the osteonal cavities by means of high-resolution SEM images, indicates that a precipitation of sulfate salts occurred, and perhaps it is still in progress, due to the enriched fluids that grow up for capillarity during the rainy period, which favored the availability of water on the surface in some areas of the museum for most of the year. As a result, fossils continue to be wet for long time, and the precipitation and dissolution cycles of salts cause mechanical damages, chemical aggression and facilitate biological attacks. The exfoliation, erosion, powdering, dissolution and endolithic attack of the bone surface, could threaten the notable scientific value of the site, hampering the development of researches. An optimal preservation of the bone surface is, for instance, the primary requirement for detecting evidence of human butchery activity on fossil bones, particularly cut marks, but also for deepened anatomo-physiological studies. Accordingly, the potential archaeological and scientific value of the palaeontological record decreases as the deterioration process increases.

All in all, this research highlights the main process affecting fossil bones after they have been uncovered, and stresses how the stabilization of the indoor environmental parameters could be regards as best protocol to reduce the damage risk of exposed bones.

ACKNOWLEDGEMENTS

We are grateful to the Dott.ssa Anna De Santis (*Soprintendenza Speciale Archeologia Belle Arti e Paesaggio di Roma*) for granting permission to carry out the research and to publish the results. We thank the teams of Laboratory of Geological Thin Sections, Laboratory of X-ray Powered diffraction and Laboratory of Electron Microscopy and Micro-analyses of the Earth Science Department, Sapienza University of Rome. We thank the HPS research group (High Pressure Spectroscopy) of the Department of Physics, Sapienza University of Rome. A particular thank to Dr Neil Helwood of Science Department (Roma 3 University) for processing the monitored environmental data.

REFERENCES

Albertano P., Moscone D., Palleschi G., Hermosin B., Saiz-Jimenez C., Sanchez-Moral S., Hernandez-Marine M., Urzi C., Groth I., Schroeckh V., Saarela M., Mattila-Sandholm T., Gallon J.R., Graziottin F., Bisconti F., Giulian R. (2003) - Cyanobacteria attack rocks (CATS): control and preventive strategies to avoid damage caused by cyanobacteria and associated microorganisms in Roman hypogean monuments. In: Saiz-Jimenez, C., (Ed), Molecular biology and cultural heritage. Swets and Zeitlinger BV, Lisse, 151-162.

Anzidei A.P., Bulgarelli G.M., Catalano P., Cerilli E., Gallotti R., Lemorini C., Milli S., Palombo M.R., Pantano W., Santucci E. (2012) - Ongoing research at the late Middle Pleistocene site of La Polledrara di Cecanibbio (central Italy), with emphasis on human-elephant relationships. Quaternary International, 255, 171-187.

Anzidei A.P., Bulgarelli G.M., Cerilli E., Fiore I., Lemorini C., Marano F., Palombo M.R., Santucci E. (2015) - Strategie di sussistenza nel Paleolitico ingeriore a La Polledrara di Cecanibbio (Roma): lo sfruttamento di una carcassa di *Palaeoloxodon antiquus*. 50° Riunione Scientifica dell'Istituto Italiano di Preistoria e Protostoria "Preistoria del Cibo", Roma 5-9 ottobre 2015, sessione 2.

Anzidei A.P., Cerilli E. (2001) - The fauna of La Polledrara di Cecanibbio and Rebibbia-Casal de' Pazzi (Rome, Italy) as an indicator for site formation processes in a fluvial environment. Proceedings of the First International Congress, The World of Elephants. Consiglio Nazionale delle Ricerche, Rome, 167-171.

Arnoldus-Huyzendveld A., Anzidei A.P. (1993) - Ricostruzione di un ambiente fluvio palustre nella regione vulcanica di Roma (La Polledrara di Cecanibbio). Paleosuperfici del Pleistocene e del primo Olocene in Italia Processi di formazione e interpretazione. Atti della XXX Riunione Scientifica Venosa e Isernia 26-29 Ottobre 1991, 151-165.

Arnoldus-Huyzendveld A., Zarlenga F., Gioia P., Palombo M.R. (2001) - Distribution in space and time and analysis of preservation factors of Pleistocene deposits in the Roman area. In: Cavarretta, G., Gioia, P., Mussi, M., Palombo, M.R. (eds.), The World of Elephants. Consiglio Nazionale delle Ricerche, Rome, 10-17.

Barbieri M., Masi U. (1978) - Considerazione geochimiche sull'origine del giacimento di Barite e Celestite di Pian dell'Organo (Civitavecchia). Società Italiana di Mineralogia e Petrologia, 34, 161-166.

Barca D., Comite V., Belfiore C.M., Bonazza A., La Russa M.F., Ruffolo S.A., Crisci G.M, Pezzino A., Sabbioni C. (2014) - Impact of air pollution in deterioration of carbonate building materials in Italian urban environments. Applied Geochemestry, 48, 122-131.

Benavente D., Sanchez-Moral S., Fernandez-Cortes A., Canaveras J.C., Elez J., Saiz-Jimenez C. (2011) - Salt damage and microclimate in the Postumius Tomb, Roman Necropolis of Carmona, Spain. Environmental Earth Science, 63, 1529-1543.

Berna F., Matthews A., Weiner S. (2004) - Solubilities of

bone mineral from archaeological sites: the recrystallization window. Journal of archaeological Science, 31, 867-882.

Biddittu I., Moncel M.H., Milli S., Bellucci L., Ruffo M., Saracino B., Manzi G. (2020) - Stratigraphy, sedimentology, and archaeology of Middle Pleistocene localities near Ceprano, Campogrande area, Italy. Quaternary Research 93, 155-171.

Brugmann G., Krause J., Brachert T.C., Kullme, O., Schrenk F., Ssemmanda I., Mertz1 D.F. (2012) - Chemical composition of modern and fossil Hippopotamid teeth and implications for paleoenvironmental reconstructions and enamel formation - Part 1: Major and minor element variation. Biogeosciences, 9, 119 -139.

Bruno L., Valle V. (2017) - Effect of white and monochromatic lights on cyanobacteria and biofilms from Roman Catacombs. International Biodeterioration and Biodegradation, 123, 286-295.

Buck L.T., Stringer C.B. (2014) - *Homo heidelbergensis*. Current Biology, 24(6), R214-R215.

Bugini R., Laurenzi Tabasso M., Realini M. (2000) - Rate of formation of black crusts on marble. A case study. Journal of Cultural Heritage, 1, 111-116.

Buzi C., Di Vincenzo F., Profico A., Manzi G. (2021) - The pre-modern human fossil record in Italy from the middle to the late pleistocene: an updated reappraisal. Alpine and Mediterranean Quaternary, 34(1), 1-16.

Caneva G., Ceschin S. (2007) - Ecologia del Biodeterioramento. In: Caneva, G., Nugari, M.P., Salvadori, O. (eds.), La Biologia Vegetale per i Beni Culturali. Biodeterioramento e Conservazione. Nardini Editore, Firenze, 35-58.

Cardell C., Benavente D., Rodríguez-Gordillo J. (2008) - Weathering of limestone building material by mixed sulfate solutions. Characterization of stone microstructure, reaction products and decay forms. Materials Characterization, 59, 1371-1385.

Castorina F., Masi U., Milli S., Anzidei A.P., Bulgarelli G.M. (2015) - Geochemical and Sr-Nd isotopic characterization of Middle Pleistocene sediments from the paleontological site of La Polledrara di Cecanibbio (Sabatini Volcanic District, central Italy). Quaternary International, 357, 253-263.

Cerilli E., Fiore I. (2018) - Natural and anthropic events at La Polledrara di Cecanibbio (Italy, Rome): some significant examples. Alpine and Mediterranean Quaternary, 31, 55-58.

Cinti D., Tassi F., Procesi M., Brusca L., Cabassi J., Capecchiacci F., Delgado Huertas A., Galli G., Grassa F., Vaselli O., Voltattorni N. (2017) - Geochemistry of hydrothermal fluids from the eastern sector of the Sabatini volcanic district (central Italy). Applied Geochemistry, 84, 187-201.

Cinti D., Vaselli O., Poncia P.P., Brusca L., Grassa F., Procesi M., Tassi F. (2019) - Anomalous concentration of arsenic, fluoride and radon in volcanic-sedimentary aquifers from central Italy: quality index for management of the water resource. Environmental Pollution, 253, 525-537.

Clementz M.T. (2012) - New insight from old bones: stable isotope analysis of fossil mammals. Journal of Mammalogy, 93, 368-380.

Combes C., Cazalbou S., Rey C. (2016) - Apatite biominerals. Minerals, 6, 34.

Decrée S., Herwart, D., Mercadier J., Miján I., de Buffrénil V., Leduc T., Lambert O. (2018) - The post-mortem history of a bone revealed by its trace element signature: The case of a fossil whale rostrum. Chemical Geology, 477, 137-150.

De Rita D., Cremisini C., Cinnirella A., Spaziani F. (2012) - Fluorine in the rocks and sediments of volcanic areas in central Italy: total content, enrichment and leaching processes and a hypothesis on the vulnerability of the related aquifers. Environmental Monitoring and Assessment, 184, 5781-5796.

Diana P., Juha S., Reinhard Z., Hervé B. (2020) - Stable isotopic and mesowear reconstructions of paleodiet and habitat of the Middle and Late Pleistocene mammals in south-western Germany. Quaternary Science Reviews, 227, 106026.

Di Sabatino B., Barrese E., Giampaolo C. (1979) - Sulla genesi delle fluoriti “sedimentarie” area meridionale del Distretto Vulcanico Sabatino. Rendiconti della società italiana di mineralogia e petrologia, 35 (1), 439-451.

Elliott J.C. (2002) - Calcium phosphate biominerals. Reviews in Mineralogy and Geochemistry, 48, 427-453.

Ferraro J.R., Nakamoto K., Brown C. (2003) - Introductory Raman Spectroscopy. 2nd edition, Academic Press, Elsevier Science.

Filippi M.L., Palombo M.R., Barbieri M., Capozza M., Iacumin P., Longinelli A. (2001) - Isotope and microwear analyses on teeth of late Middle Pleistocene *Elephas antiquus* from the Rome area (La Polledrara, Casal de’ Pazzi). In: Cavarretta C., Gioia P., Mussi M., Palombo M.R. (eds.), Proceedings of the First International Congress, The World of Elephants. Consiglio Nazionale delle Ricerche, Rome, 534-539.

Gallego-Cartagena E., Morillas H., Maguregui M., Patiño-Camelo K., Marcaida I., Morgado-Gamero W., Silva L.F.O., Madariaga J.M. (2020) - A comprehensive study of biofilms growing on the built heritage of a Caribbean industrial city in correlation with construction materials. International Biodeterioration and Biodegradation, 147, 104874.

Goldstein J.I., Newbury D.E., Joy D.C., Lyman C.E., Echlin P., Lifshin E., Sawyer L., Michael J. (2018) - Scanning electron microscopy and X-ray microanalysis. 4th ed. New York: Springer.
Doi: 10.1007/978-1-4939-6676-9

Hanegraef H., Martinón-Torres M., Martínez de Pinillos M., Martín-Francés L., Vialet A., Arsuaga J.L., Bermúdez de Castro J.M. (2018) - Dentine morphology of Atapuerca-Sima de los Huesos lower molars: Evolutionary implications through three-dimensional geometric morphometric analysis. American Journal of Physical Anthropology, 166(2), 276-295.

Hanor J.S. (2000) - Barite-celestine geochemistry and environments of formation. Reviews in Mineralogy and Geochemistry, 40, 193-275.

Hubert J.F., Panish P.T., Chure D.J., Prostak K.S. (1996) - Chemistry, microstructure, petrology, and diagenetic model of Jurassic dinosaur bones, Dinosaur National Monument, Utah. Journal of Sedimentary Research, 66, 531-547.

Jaouen K. (2018) - What is our toolbox of analytical chemistry for exploring ancient hominin diets in the absence of organic preservation? Quaternary Science Reviews, 197, 307-318.

Jaouen K., Pons M.L. (2017) - Potential of non-traditional isotope studies for bioarchaeology. Archaeological and Anthropological Sciences, 9, 1389-1404.

Keenan S.W., Engel A.S., Roy A., Bovenkamp-Langlois G.L. (2015) - Evaluating the consequences of diagenesis and fossilization on bioapatite lattice structure and composition. Chemical Geology, 413, 18-27.

Keenan S.W. (2016) - From bone to fossil: A review of the diagenesis of bioapatite. American Mineralogist, 101, 1943-1951.

Kohn M.J., Law J.M. (2006) - Stable isotope chemistry of fossil bone as a new paleoclimate indicator. Geochimica et Cosmochimica Acta, 70, 931-946.

Korkang M., Savran A. (2015) - Impact of the surface roughness of stone used in historical buildings and biodeterioration. Constructing and Building Materials, 80, 279-294.

Kühl G., Nebergall W.H. (1963) - Hydrogenphosphat- und Carbonatapatite. Zeitschrift für Anorganische und Allgemeine Chemie, 324, 313-320.

Kumar N., Weckhuysen B.M., Wain A.J., Pollard A.J. (2019) - Nanoscale chemical imaging using tip-enhanced Raman spectroscopy. Nature protocols, 14(4), 1169-1193.

Lee-Thorp J. (2002) - Two decades of progress towards understanding fossilization processes and isotopic signals in calcified tissue minerals. Archaeometry, 44, 435-446.

Lepinay C., Mihajlovski A., Touron S., Seyer D., Bousta F., Di Martino P. (2018) - Bacterial diversity associated with saline efflorescences damaging the walls of a French decorated prehistoric cave registered as a World Cultural Heritage Site. International Biodeterioration and Biodegradation, 130, 55-64.

Leroy N., Bres E. (2001) - Structure and substitutions in fluorapatite. European Cells and Materials, 2, 36-48.

Lopez-Arce P., Fort-Gonzales R., Gomez-Hers M., Pérez-Monserrat E.M., Varas M.J. (2011) - Preservation strategies for avoidance of salt crystallization in El Paular Monastery Cloister, Madrid, Spain. Environmental Earth Sciences, 63, 1487-1509.

Ma J., Wang Y., Jin C.Z., Zhang H.W., Hu Y.W. (2019) - A preliminary study of serial stable isotope analysis tracks foraging ecology of fossil Asian elephants in South China. Vertebrata PalAsiatica, 57, 225-240.

Mallouchou M.S., Stathopoulou E.T., Theodorou G.E. (2018) - How Do Fossilized Mammalian Bones Behave During Chemical Conservation? The Histological Case Studies of Tilos and Kerassia. Geoheritage, 11, 597-614.

Manthi F.K., Cerling T.E., Chritz K.L., Blumenthal S.A. (2020) - Diets of mammalian fossil fauna from Kanapoi, northwestern Kenya. Journal of Human Evolution, 140, 102338.

Manzi G. (2016) - Humans of the Middle Pleistocene: The controversial calvarium from Ceprano (Italy) and its significance for the origin and variability of *Homo heidelbergensis*. Quaternary International, 411, 254-261.

Manzi G., Magri D., Milli S., Palombo M.R., Celiberti V., Margari V., Barbieri M., Barbieri M., Melis R.T., Rubini M., Ruffo M., Saracino B., Tzedakis P.C., Zarattini A, Biddittu I. (2010) - The new chronology of the Ceprano calvarium (Italy). Journal of Human Evolution, 59, 580-585.

Marano F., Di Rita F., Palombo M.R., Ellwood N.T.W., Bruno L. (2016) - A first report of biodeterioration caused by cyanobacterial biofilms of exposed fossil bones: A case study of the Middle Pleistocene site of La Polledrara di Cecanibbio (Rome, Italy). International Biodeterioration and Biodegradation, 106, 67-74.

Mastrangelo F. (1976) - I giacimenti. Rendiconti della Società Italiana di Mineralogia e Petrologia, 32, 29-46.

Matteucci E. (1976) - Le fluoriti sedimentarie laziali: ipotesi e problemi genetici. Rendiconti della Società Italiana di Mineralogia e Petrologia, 32, 47-63.

McLaughlin G., Lednev I.K. (2011) - Potential application of Raman spectroscopy for determining burial duration of skeletal remains. Analytical and bioanalytical chemistry, 401, 2511-2518.

Merk V., Berg J.K., Krywka C., Burget I. (2017) - Oriented crystallization of Barium Sulfate confined in hierarchical cellular structures. Crystal Growth Design, 17, 677-684.

Miller A.Z., Liaz L., Dionisio A., Macedo M.F., Saiz-Jimenez C. (2009) - Growth of phototrophic biofilms from limestone monuments under laboratory conditions. International Biodeterioration and Biodegradation, 63, 860-867.

Milli S., Palombo M.R., Anzidei A.P. (2011) - I depositi pleistocenici di Ponte Galeria e la Polledrara di Cecanibbio. In: Guidebook Post-congress Field Trip. AIQUA 2011 "Il quaternario Italiano - Conoscenze e prospettive". Italian Association for Quaternary Studies, Rome. February 26, pp. 37.

Nielsen-Marsh C.M., Hedges R.E. (2000) - Patterns of diagenesis in bone I: the effects of site environments. Journal of Archaeological Science, 27, 1139-1150.

Owens C.L., Nash G.R., Hadler K., Fitzpatrick R.S., Anderson C.G., Wall F. (2019) - Apatite enrichment by rare earth elements: a review of the effect s of surface properties. Advances in colloid and interface science, 265, 14-28.

Palombo M.R., Filippi M.L., Iacumin P., Longinelli A., Barbieri M., Maras A. (2005) - Coupling tooth microwear and stable isotope analyses for palaeodiet reconstruction: the case study of Late Middle Pleistocene *Elephas* (*Palaeoloxodon*) *antiquus* teeth from Central Italy (Rome area). Quaternary International, 126-128, 153-170.

Palombo M.R., Cerilli E. (in press) - Human-elephant interactions during the Lower Palaeolithic: scrutini-

zing the role of environmental factors. In: Harvati K Konidaris G., Barkai R., Kießling K. (Eds), The Human-Elephant Interactions from Past to Present. Tübingen University Press (2020).

Pasteris J.D., Ding D.Y. (2009) - Experimental fluoridation of nanocrystalline apatite. American Mineralogist, 94, 53-63.

Pate F.D., Hutton J.T., Norrish K. (1989) - Ionic exchange between soil solution and bone: toward a predictive model. Applied Geochemistry, 4, 303-316.

Pereira A., Nomade S., Faulguères C., Bahain J.J., Tombret O., Garcia T., Voichet P., Bulgarelli G.M., Anzidei A.P. (2017) - 40Ar/39Ar and ESR/U-series data for the La Polledrara di Cecanibbio archaeological site (Lazio, Italy). Journal of Archaeological Science, Reports, 15, 20-29.

Piga G., Santos-Cubedo A., Brunetti A., Piccinini M., Malgosa A., Napolitano E., Enzo S. (2011) - A multitechnique approach by XRD, XRF, FT-IR to characterize the diagenesis of dinosaur bones from Spain. Palaeogeography, Palaeoclimatology, Palaeoecology, 310, 92-107.

Piga G., Santos-Cubedo A., Moya Solà S., Brunetti A., Malgosa A., Enzo S. (2009) - An X-ray Diffraction (XRD) and X-ray Fluorescence (XRF) investigation in human and animal fossil bones from Holocene to Middle Triassic. Journal of Archaeological Science, 36, 1857-1868.

Rijniers A.L., Pel L., Huinink H.P., Kopinga K. (2005) - Salt crystallization as damage mechanism in porous building materials - a nuclear magnetic resonance study. Magnetic Resonance Imaging, 23, 273-276.

Roksandic M., Radović P., Lindal J. (2018) - Revising the hypodigm of *Homo heidelbergensis*: A view from the Eastern Mediterranean. Quaternary International, 466, 66-81.

Roksandic M., Radović P., Wu X., Bae C. (2019) - Homo heidelbergensis: What do we need to set the question of the validity of this taxon to rest. American Journal of Physical Anthropology, 168, 207-207.

Rodriguez-Navarro C., Doehne E. (1999) - Salt weathering: influence of evaporation rate, supersaturation and crystallization pattern. Earth Surface Processes and Landform, 24, 191-209.

Rollin-Martinet S., Navrotsky A., Champion E., Grossin D., Drouet C. (2013) - Thermodynamic basis for evolution of apatite in calcified tissues. American Mineralogist, 98, 2037-2045.

Santucci E., Marano F., Cerilli E., Fiore I., Lemorini C., Palombo M.R., Anzidei A.P., Bulgarelli G.M. (2016) - *Palaeoloxodon* exploitation in the late Middle Pleistocene site of Polledrara di Cecanibbio (Rome, Italy). Quaternary International, 406, 169-182.

Silaev V.I., Ponomarev D.V., Kiseleva D.V., Smoleva I.V., Simakova Y.S., Martirosyan O. V., Vasilev A., Khazov F., Tropnikov E.M. (2017) - Mineralogical-geochemical characteristics of the bone detritus of Pleistocene mammals as a source of paleontological information. Paleontological Journal, 51, 1395-1421.

Stringer C. (2012) - The status of *Homo heidelbergensis* (Schoetensack 1908). Evolutionary Anthropology: Issues, News, and Reviews, 21(3), 101-107.

Suarez M.B., Passey B.H. (2014) - Assessment of the clumped isotope composition of fossil bone carbonate as a recorder of subsurface temperatures. Geochimica et Cosmochimica Acta, 140, 142-159.

Suarez C.A., Kohn M.J. (2020) - Caught in the act: A case study on microscopic scale physicochemical effects of fossilization on stable isotopic composition of bone. Geochimica et Cosmochimica Acta, 268, 277-295.

Thomas D.B., Fordyce R.E., Frew R.D., Gordon K.C. (2007) - A rapid, non-destructive method of detecting diagenetic alteration in fossil bone using Raman spectroscopy. Journal of Raman Spectroscopy, 38, 1533-1537.

Thomas D.B., McGoverin C.M., Fordyce R.E., Frew R.D., Gordon K.C. (2011) - Raman spectroscopy of fossil bioapatite - A proxy for diagenetic alteration of the oxygen isotope composition. Palaeogeography, Palaeoclimatology, Palaeoecology, 310, 62-70.

Tomaselli L., Tiano P., Lamenti G. (2000) - Occurrence and fluctuation in photosynthetic biocoenoses dwelling on stone monuments. In: Ciferri O., Tiano P., Mastromei G. (Eds), Of Microbes and Art - The Role of Microbial Communities in the Degradation and Protection of Cultural Heritage, 63 - 76. New York: Kluwer.

Trueman C.N.G., Tuross N. (2002) - Trace elements in recent and fossil bone apatite. Reviews in mineralogy and geochemistry, 48, 489-521.

Trueman C.N.G., Behrensmeyer A.K., Turos N., Weiner S. (2004) - Mineralogical and compositional changes in bones exposed on soil surfaces in Amboseli National Park, Kenya: diagenetic mechanisms and the role of sediment pore fluids. Journal of Archaeological Science, 31, 721-739.

Vijayakumar S. (2014) - Role of Cyanobacteria In Biodeterioration of Historical Monuments - A Review. BMR Microbiology, 1, 1-13.

Winand L. (1961) - Etude physico-chimique du phosphate tricalcique hydrate et de l'hydroxylapatite. Annales de Chimie (Paris), 6, 941-967.

Zammit G., Sanchez-Moral S., Albertano P. (2011) - Bacterially mediated mineralization processes lead to biodeterioration of artworks in Maltese catacombs. Science of Total Environment, 409, 2773-2782.

Zong C., Xu M., Xu L.J., Wei T., Ma X., Zheng X.S., Ren H., Ren B. (2018) - Surface-Enhanced Raman Spectroscopy for Bioanalysis: Reliability and Challenges. Chemical Reviews, 118(10), 4946-4980.

Ms. received: 11 October, 2020 *Revised: 30 April, 2020*
Accepted: 07 May, 2021 *Avaiable online: 21 June, 2021*